Supporting Information

Agafonov *et al.* 10.1073/pnas.0801342105

SI Text

Binding of Nucleotide. Analogs to IASL-S1. Addition of 5 mM nucleotide analog to IASL-S1 under EPR conditions (as in Table 2) abolished virtually all myosin ATPase activity (Table S1), showing that IASL-S1 is saturated with these nucleotide analogs. This justifies our treating these complexes as distinct and homogeneous biochemical states.

Sensitivity of EPR Spectra to ADP. Fig. S1 shows EPR spectra in the apo and ADP-bound states of myosin. Although at first glance these spectra appear to show little or no effects of ADP, *Insets* show the expanded low-field and high-field peaks, which show clear ADP effects. This is important, because the splitting between the outer extrema can be used to quantitate spin-label mobility. In particular, the order parameter (assuming subnanosecond rotational motion) can be calculated accurately from $S = (T_{\parallel}' - T_0)/(T_{\parallel} - T_0)$, where $2T_{\parallel}'$ is the observed splitting between the outer peaks, $2T_{\parallel}$ is the splitting for a completely immobilized label (frozen sample), and $2T_0$ is the isotropic splitting (free spin label in solution) (1). In both muscle and *Dicty*, ADP produces a narrower splitting, indicating increased spin-label mobility (decreased order parameter) in this state. The position of each peak can typically be determined with an accuracy of 0.1 G or less, so the value of the splitting ($2T_{\parallel}'$) can be determined with precision ±0.2 G. As the table in Fig. S1 shows, there are no significant differences between muscle and *Dicty*, but in both cases, the observed decrease in splitting due to ADP is quite significant and reflects a significant decrease in order parameter S and thus a change in myosin structure (opening of the spin label-binding pocket) upon ADP binding (Fig. S1).

Temperature Dependence of the M*–M Transition: Calculation of Thermodynamic Parameters.** EPR spectra $V_{exp}(H)$ of myosin complexes with nucleotide analogs were recorded at different temperatures and deconvoluted to extract the mole fractions x* and x** of the spectral components corresponding to the M* and M** structural states (2) according to

$$V_{exp}(H) = x^*V^*(H) + x^{**}V^{**}(H), \qquad [S1]$$

where $x^* = [M^*]/[M^* + M^{**}]$ and $x^{**} = 1 - x^*$ (Fig. S2). These mole fractions were then used to calculate the equilibrium constant K_{eq} for the reaction:

$$M^* \rightarrow M^{**}, \qquad K_{eq} = [M^{**}]/[M^*] = x^{**}/x^*. \qquad [S2]$$

ΔG was calculated as $-RT \ln K_{eq}$, and the change in entropy (ΔS) and enthalpy (ΔH) between the two conformations was found by fitting the data with the the van't Hoff equation,

$$\ln K_{eq} = \Delta S/R - \Delta H/(RT), \qquad [S3]$$

as illustrated in Fig. S3 and Table S2.

ATPase Assays. High-salt ATPase activity (reported in Table 1) was measured by phosphate liberation (3) at $T = 25$°C in buffers containing 50 mM Mops, 5 mM EDTA, 0.6 M KCl (pH 7.5) for K/EDTA ATPase, and 50 mM Mops, 10 mM $CaCl_2$, 0.6 M KCl (pH 7.5) for Ca/K ATPase (3). Myosin ATPase activity was measured under physiological conditions [$T = 25$°C in 10 mM Tris, 3 mM $MgCl_2$, 2.5 mM ATP (pH 7.5)] in the presence and absence of actin, by the liberation of inorganic phosphate (3, 4). The dependence of S1 ATPase activity on actin concentration was fitted to the Michaelis–Menten equation, to determine V_{max} (activity at saturating actin) and K_m (actin concentration when $v = 0.5\ V_{max}$), as reported in Table 2. Mg^{2+} ATPase activity of IASL-S1 nucleotide analog-bound complexes was measured at $T = 25$°C in buffer containing 20 mM EPPS (pH 8.0), 6 mM $MgCl_2$, 1 mM EGTA, 5 mM ATP by the liberation of inorganic phosphate (3), as reported in Table S1.

1. Squier TC, Thomas DD (1989) Selective detection of the rotational dynamics of the protein-associated lipid hydrocarbon chains in sarcoplasmic reticulum membranes. *Biophys J* 56:735–748.
2. Nesmelov YE, Agafonov RV, Burr A, Weber RT, Thomas DD (2008). Structure and dynamics of the force generating domain of myosin probed by multifrequency electron paramagnetic resonance. *Biophys J* 95:247–256.
3. Lanzetta PA, Alvarez LJ, Reinach PS, Candia OA (1979) An improved assay for nanomole amounts of inorganic phosphate. *Anal Biochem* 100:95–97.
4. Fiske CHS, Y (1925). The calorimetric determination of phosphorus. *J Biol Chem* LXVI:375–400.

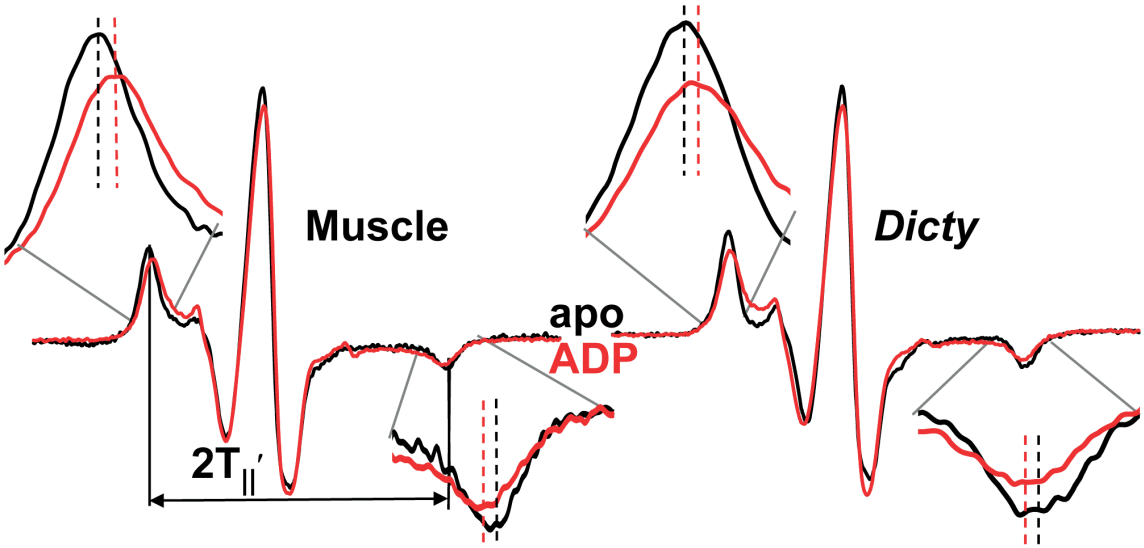

	Muscle		*Dicty*	
	$2T_{\|\|}'$	S	$2T_{\|\|}'$	S
apo	67.6 ± 0.2	0.957 ± 0.004	67.8 ± 0.2	0.960 ± 0.004
ADP	66.4 ± 0.2	0.936 ± 0.004	66.8 ± 0.2	0.943 ± 0.004

Fig. S1. EPR spectra of muscle (*Left*) and *Dicty* (*Right*) S1 in apo and ADP-bound states.

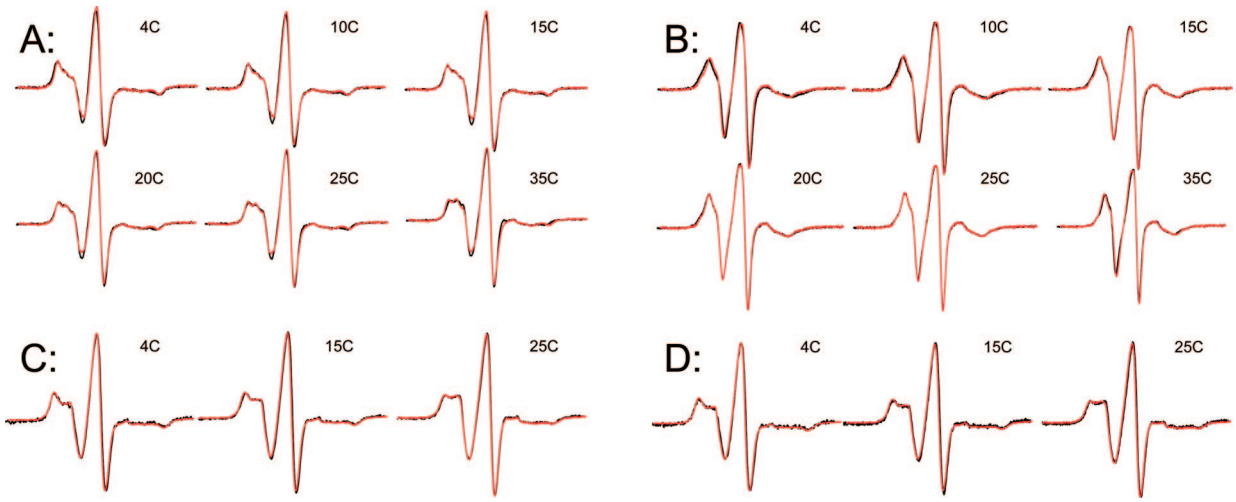

Fig. S2. EPR spectra at different temperatures, fit to a sum of M* and M** components (Eq. **S1**) obtained at the same temperature. Black, experiment; red, best-fit simulation. (*A* and *B*) Muscle myosin. (*C* and *D*) *Dicty* myosin. (*A* and *C*) Prehydrolysis analog (ADP.BeF_x). (*B* and *D*) Posthydrolysis analog (ADP.AlF_4).

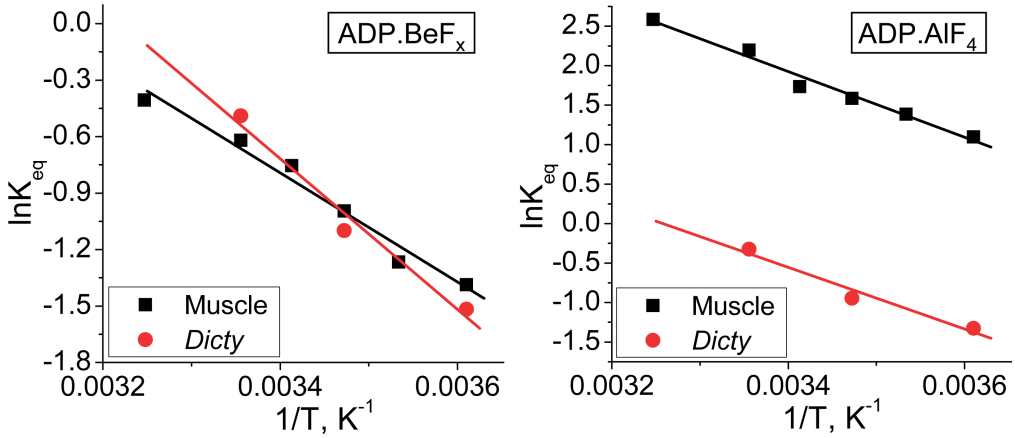

Fig. S3. Van't Hoff plots for the reaction M* → M** (recovery stroke), for muscle and *Dicty* myosins complexed with ADP.BeF$_x$ (*Left*) and ADP.AlF$_4$ (*Right*). K_{eq} was determined from deconvolution of EPR spectra (Fig. S2), using Eqs. **S1** and **S2**. Values for ΔH and ΔS, given in Table S2, were determined by fitting the data to Eq. **S3**, so the *y*-intercept is $\Delta S/R$, and the slope is $-\Delta H/R$.

Table S1. Mg-ATPase activity of S1 nucleotide analog complexes

Myosin	M.ADP.AlF_4, %	M.ADP.BeF_x, %	M.ADP.V, %
Muscle	1.4 ± 0.3	0.5 ± 0.4	3.2 ± 1.6
Dicty	0.2 ± 0.3	0	3.4 ± 0.7

100% corresponds to the value in the absence of nucleotide analog (Table 2, V_{basal}, labeled).

Table S2. Enthalpy (Δ*H*) and entropy (Δ*S*) change in the transition from the M* to M structural state (recovery stroke) in myosin complexed with nucleotide analogs**

	ADP.BeF$_x$		ADP.AlF$_4$	
	ΔH, kcal/mol	ΔS, kcal/(mol·K)	ΔH, kcal/mol	ΔS, kcal/(mol·K)
Muscle	6.0 ± 0.5	0.018 ± 0.002	8.4 ± 0.6	0.032 ± 0.002
Dicty	7.8 ± 1.2	0.026 ± 0.004	7.8 ± 1.5	0.025 ± 0.005